TU Delft

Delft University of Technology

Thermally self-sufficient process for cleaner production of e-methanol by CO_2 hydrogenation

Vaquerizo, Luis; Kiss, Anton A.

DOI
10.1016/j.jclepro.2023.139845

Publication date
2023

Document Version
Final published version

Published in
Journal of Cleaner Production

Citation (APA)
Vaquerizo, L., & Kiss, A. A. (2023). Thermally self-sufficient process for cleaner production of e-methanol by CO_2 hydrogenation. *Journal of Cleaner Production*, *433*, Article 139845. https://doi.org/10.1016/j.jclepro.2023.139845

Important note
To cite this publication, please use the final published version (if applicable).
Please check the document version above.

Copyright
Other than for strictly personal use, it is not permitted to download, forward or distribute the text or part of it, without the consent of the author(s) and/or copyright holder(s), unless the work is under an open content license such as Creative Commons.

Takedown policy
Please contact us and provide details if you believe this document breaches copyrights.
We will remove access to the work immediately and investigate your claim.

This work is downloaded from Delft University of Technology.
For technical reasons the number of authors shown on this cover page is limited to a maximum of 10.

Journal of Cleaner Production 433 (2023) 139845

Contents lists available at ScienceDirect

Journal of Cleaner Production

journal homepage: www.elsevier.com/locate/jclepro

Thermally self-sufficient process for cleaner production of e-methanol by CO_2 hydrogenation

Luis Vaquerizo [a,b], Anton A. Kiss [b,*]

[a] Institute of Bioeconomy, PressTech Group, Department of Chemical Engineering and Environmental Technology, University of Valladolid, Doctor Mergelina s/n, 47011, Valladolid, Spain
[b] Department of Chemical Engineering, Delft University of Technology, Van der Maasweg 9, 2629 HZ, Delft, the Netherlands

ARTICLE INFO

Handling Editor: Panos Seferlis

Keywords:
Process integration
Optimal process design
Dividing-wall column
Energy efficiency

ABSTRACT

The hydrogenation of CO_2 to methanol is a technology that converts a greenhouse gas into a valuable chemical compound that efficiently stores energy. Several alternatives to perform this process have been proposed, but they are either not thermally self-sufficient and depend on using external fuel, or the power usage per ton of methanol is insufficiently optimized, or part of the raw materials must be purged and therefore there is a loss of methanol yield.

This original study aims to develop a novel thermally self-sufficient process for e-methanol production (at practically 100% yield along with water by-product of 0.37 $kg_{water}/kg_{product}$) that only uses green electricity. The main innovation of the process is an effective thermally self-sufficient heat-integration scheme that only needs 0.0059 $m^3_{water}/kg_{methanol}$ combined with using a dividing wall column to recover the unreacted CO_2 and obtain high purity methanol. In addition, the pressure reduction in the reaction-separation loop is limited to the pressure drop of the circuit to minimize the overall green electricity use to only 656 kWh per ton methanol, resulting in net CO_2 emissions of −1.13 kg_{CO2}/kg_{MeOH} or 0.78 kg_{CO2}/kg_{MeOH} when the plant operates with green or grey hydrogen and electricity, respectively. Finally, the operating pressure in the reactor is optimized at 65 bar to minimize the total annualized cost.

1. Introduction

The catalytic conversion of waste CO_2 into methanol is an opportunity to reduce greenhouse gas emissions that contribute to climate change and ocean acidification while generating a valuable chemical compound (Porosoff et al., 2016). CO_2 is an inexpensive C1 source that can be converted into methanol by hydrogenation, to efficiently store the energy used to produce hydrogen by water electrolysis. Although hydrogen has a high energy storage capacity per unit of mass, its low density at standard conditions (0.08 kg/m^3) or even in liquid phase (70.85 kg/m^3 at 20 K) makes its storage and transportation difficult (Lee et al., 2020).

The production of methanol by CO_2 hydrogenation has been intensively studied during the past years, with many reviews covering this topic. Dieterich et al. (2020) showed the historical evolution of the methanol production process and did a benchmarking analysis between the existing technologies focusing on the catalyst used, the reaction temperature and pressure, and the rector configuration, concluding that, for methanol production from CO_2 and hydrogen, long-term studies are still needed to determine catalyst deactivation and the optimal operating conditions, and new catalysts need to be developed to increase methanol yield and reduce the problems caused by increased water production since the existing industrial production processes still rely on the conventional Cu/Zn/Al and $CuO/ZnO/Al_2O_3$ catalysts. Bowker (2019) discussed the differences between a traditional methanol production plant and a renewable methanol plant stating that, in a green methanol plant, hydrogen must be produced by water electrolysis using green electricity mainly from wind or solar power production plants, heat recovery must be maximized and that the selection of the technology used for the separation of methanol from water must be carefully addressed because of the higher water content at the outlet of the reactor. Professor Demirel's research group performed life cycle analysis for methanol production using CO_2 from different sources, such as an ethanol production plant by fermentation (Matzen et al. (2015a, 2015b & 2016) and a coal oxy-combustion plant. They concluded that the hydrogen production cost is the major cost driver of the process and

* Corresponding author.
E-mail addresses: A.A.Kiss@tudelft.nl, tonykiss@gmail.com (A.A. Kiss).

https://doi.org/10.1016/j.jclepro.2023.139845
Received 4 July 2023; Received in revised form 22 October 2023; Accepted 18 November 2023
Available online 23 November 2023
0959-6526/© 2023 The Authors. Published by Elsevier Ltd. This is an open access article under the CC BY license (http://creativecommons.org/licenses/by/4.0/).

therefore, that more research is needed in electrolysis technologies, that a reduction of around 85% of greenhouse gas emissions is possible when compared with fossil-fuel ethanol production, and that further work is needed to convert methanol into value-added chemicals. Dang et al. (2019) reviewed different types of heterogeneous catalysts stating that the development of more efficient catalysts will allow for decreasing the operating temperature in the reactor, increasing the equilibrium conversion. In this sense, metal-based catalysts show higher activity, selectivity and stability when compared with oxide catalytic systems. Kanuri et al. (2022) reviewed the effect of the different process parameters on the overall process yield and also remarked that when designing an efficient catalyst, the thermomechanical stability of the catalyst plays a major role. Zhong et al. (2020) pointed out that compared with the conventional methanol process from syngas, CO_2 hydrogenation requires more hydrogen and that the thermodynamics of CO_2 hydrogenation are less favorable than those of CO. Moreover, they compared different types of heterogeneous catalysts and showed the recent advances in reactor design. Finally, Ren et al. (2022) focused on the design of novel catalysts for CO_2 hydrogenation into methanol concluding that catalyst development at a larger size, including the analysis of activity and stability, may fasten the industrialization objective.

During the last few years, several authors have proposed different process alternatives seeking to find the most efficient and environmentally sustainable option. Kiss et al. (2012, 2016) presented a process that uses a dual-function stripper to efficiently recover CO/CO_2 from the methanol-water mixture while removing the water from the wet hydrogen feed stream, improving the equilibrium conversion in the hydrogenation reaction. The process was not thermally self-sufficient since it required 254 kWh of heat per ton of MeOH in the reboiler of the methanol-water distillation column. GhasemiKafrudi et al. (2022) substituted the catalyst used in the process of Kiss et al. (2012,2016) with the most efficient $CuZnOAl_2O_3$ catalyst that allows for a slight reduction of the recycling flowrate, power and steam consumption (522 vs 550 kWh/ton of methanol in Kiss et al. (2012, 2016). However, the process was still not thermally self-sufficient as it still required 89 kWh of external heat per ton of methanol in the reboiler of the methanol-water distillation column. Lonis et al. (2021) and Sollai et al. (2023) proposed a thermally self-sufficient process, but in this process, there is a purge, so the overall methanol yield decreases to 95%, while the catalyst load is much higher (73 vs 8.7 $kg_{catalyst}$/kton/year MeOH in Kiss et al. (2016). Meunier et al. (2020) and Pérez-Fortes et al. (2016) also proposed thermally self-sufficient processes, but the main drawback was that both processes required much more catalyst in the reactor (303 & 101 vs 8.7 $kg_{catalyst}$/kton/year MeOH in Kiss et al. (2016). Moreover, in both processes, the methanol yield was lower than 95% as compared to 99.83% in Kiss et al. (2016). Finally, Wang et al. (2023) recently presented a thermally self-sufficient process that included a double-effect distillation process. In their work, the catalyst load is also much higher (216 vs 8.7 $kg_{catalyst}$/kton/year MeOH in Kiss et al. (2016), and two classic distillation columns of 40 and 30 trays are required, as compared with a stripper of 4 trays and a distillation column of 30 trays in Kiss et al. (2016).

Although some thermally self-sufficient process alternatives have been already proposed, there is still a lack of an e-methanol production process that uses a small amount of catalyst per kton of MeOH produced, has no waste of reactants (maximized methanol yield, minimizes the compressors power, and reduces the use of multiple columns. This work aims to develop an efficient process alternative that does not require the use of an external fuel for heat generation, that minimizes power consumption and that maximizes the process yield. Although this approach is challenging and difficult, it is also very much needed to boost the profitability and environmental sustainability of the process. Although some alternative promising technologies such as methanol production by plasma catalysis have been proposed to enable CO_2 conversion into methanol at ambient conditions (Liu et al., 2019), they still have not reached the required level of maturity for their industrial implementation.

This article is the first to present a novel thermally self-sufficient energy-integrated process for clean e-methanol production by CO_2 hydrogenation, using an effective heat-integration, a single-step fluid separation in a dividing wall column (DWC) that allows the recovery of all unreacted CO_2 and obtaining high purity methanol at the maximum possible (stoichiometric) yield, and with best-in-class power consumption due to high pressure operation along the reaction-separation-recycle (RSR) loop. The results are provided for a 100 ktpy methanol plant capacity basis, which allows a direct comparison with previous work from literature (Kiss et al., 2016; GhasemiKafrudi et al., 2022; Wang et al., 2023). While hydrogen will be produced by water electrolysis using electricity from wind or solar power plants, CO_2 will be captured from the flue gas of an energy-intensive chemical industry such as a petrochemical complex, an ammonia production plant, or a cement production plant. This is preferred in comparison with other CO_2 sources such as combined cycle power production plants because of the lower fluctuation in the CO_2 supply rate. Another option is to use the CO_2 by-product from bioethanol production plants. The lower cost of this CO_2 (considered as beverage grade) can help in the reduction of the minimum selling price of methanol.

2. Problem statement

The environmental sustainability of methanol by CO_2 hydrogenation process strongly depends on using only green electricity as the power source and not depending on the consumption of external fuels for heat production, as this would generate additional CO_2 emissions (Lee et al., 2020). Although several improved process alternatives have been proposed in the past years, either they depend on external heat sources or the power consumption is not optimal, or part of the raw materials are purged from the process, meaning that there are CO_2 emissions and/or waste of green hydrogen. To address these crucial issues, a thermally self-sufficient process is proposed here, in which the pressure drop in the reaction-separation-recyle loop is kept to a minimum (to reduce the power consumption in the recycling compressor), there is no purge whatsoever, such that the CO_2 conversion yield is maximized, and the use of a DWC (Kiss, 2012) recovers all the unreacted CO_2 (in the top product) and allows obtaining high purity methanol product as side-stream and water as bottom product.

3. Basic data

This section presents the simulation basis for a plant of 100 ktpy of methanol by CO_2 hydrogenation. To allow a direct comparison with the results obtained by Kiss et al. (2016), the same fibrous Cu/Zn/Al/Zr (An et al., 2009) catalyst is considered in this work, which is very similar to commercial catalysts.

3.1. Property model

The process was rigorously simulated in Aspen Plus using the fugacity-activity coefficient approach in line with literature recommendations (Dimian et al., 2014, 2019). Peng Robinson Equation of State (PR-EOS) was selected to model the vapor phase due to the high operating pressures and temperatures (pressure up to 65 bar and temperature up to 250 °C), and the non-random two-liquid activity coefficient model (NRTL) was chosen to model the liquid phase due to the polar nature of the liquid compounds (H_2O and CH_3OH). All the binary interaction parameters required for both the PR-EOS and the NRTL model are available in the Aspen Plus databanks (e.g. APV-120 ENRTL-RK, APV-120 VLE-RK and APV-120 EOS-LIT).

3.2. Chemical reactions

The chemistry of methanol production by CO_2 hydrogenation involves three main equilibrium reactions (A, B and C). Water is also produced as a by-product (Fiedler et al., 2005):

$$A)\ CO + 2\ H_2 \leftrightarrows CH_3OH\ \Delta H_{298K} = -90.77\ kJ/mol \quad (1)$$

$$B)CO_2 + H_2 \leftrightarrows CO + H_2O\ \Delta H_{298K} = +41.21\ kJ/mol,\ \text{Reverse water-gas shift (WGS) reaction} \quad (2)$$

$$C)CO_2 + 3\ H_2 \leftrightarrows CH_3OH + H_2O\ \Delta H_{298K} = -49.16\ kJ/mol \quad (3)$$

As widely explained in previous research and reviews, for example in Dimian et al. (2019) and Kanuri et al. (2022), higher methanol yields are obtained at lower reaction temperatures and higher reaction pressures. Moreover, for this process the optimum stoichiometric number (SN) is equal to 2, meaning a molar (H_2/CO_2) feed ratio of 3:1 when only CO_2 and H_2 are present. While a higher stoichiometric number means an excess of hydrogen in the feed, stoichiometric numbers lower than 2 mean an excess of carbon. The SN number is calculated as follows:

$$SN = \frac{y_{H_2} - y_{CO_2}}{y_{CO} + y_{CO_2}} \quad (4)$$

3.3. Chemical equilibrium

The values for the equilibrium constants (K_A, K_B and K_C) used in this work were reported by Lim et al. (2009), using the experimental data from Graaf et al. (1986) but providing an explicit model consistent with the requirements for process simulations in Aspen Plus. Kiss et al. (2016) compared the literature data from Lim et al. (2009) with the equilibrium constant data obtained using an equilibrium reaction in Aspen Plus, showing an excellent agreement. The equilibrium constants are presented hereafter, also as [Pa] based correlations as they are required in this form when implemented in the driving force term of the kinetic equations.

$$\ln K_A = \frac{9.8438 \times 10^4}{RT} - 29.07 \rightarrow K_A = 2.3717 \times 10^{-13} \exp\left(\frac{9.8438 \times 10^4}{RT}\right)\ [atm^{-2}]$$

$$\ln K_A = -52.096 + \frac{11840}{T};\ with\ K_A\ [Pa^{-2}] \quad (5)$$

$$\ln K_B = \frac{-4.3939 \times 10^4}{RT} + 5.639 \rightarrow K_B = 2.8118 \times 10^2 \exp\left(\frac{-4.3939 \times 10^4}{RT}\right)[-]$$

$$\ln K_B = 5.639 + \frac{-5285}{T};\ with\ K_B\ [-] \quad (6)$$

$$K_C = K_A \times K_B \rightarrow K_C = 6.6688 \times 10^{-11} \exp\left(\frac{5.4499 \times 10^4}{RT}\right)\ [atm^{-2}]$$

$$\ln K_C = -46.457 + \frac{6555}{T};\ with\ K_C\ [Pa^{-2}] \quad (7)$$

3.4. Catalyst and kinetics

This work uses the catalyst and kinetic model from Kiss et al. (2016). Briefly, this model is based on the A3B2C3 kinetic model tested by Graaf et al. (1986) combined with the kinetic data from An et al. (2009). The experimental data from An et al. (2009) was obtained for a fibrous Cu/Zn/Al/Zr catalyst specially designed for CO_2 hydrogenation. For details on how to implement this model in Aspen Plus and its validation, refer to Kiss et al. (2016). Although the kinetic model is only intended to be used at reaction pressures below 50 bar, the model was tested at reaction pressures up to 70 bar using the experimental data from Park et al. (2015). The good agreement between the experimental data and the model predictions (less than 5% error, Table 4) validates the use of the kinetic model also at these operating pressures.

All the required input data for the kinetic equations using the Aspen Plus format are provided in Table 1, Table 2 and Table 3. The corresponding rate equations for the kinetic model, implemented in Aspen Plus as Langmuir-Hinshelwood-Hougen-Watson (LHHW) kinetics in a plug flow reactor, are:

$$r_{CH_3OH,A3} = k_A \frac{K_{CO}\left[f_{CO} {f_{H_2}}^{3/2} - f_{CH_3OH} \Big/ \left(K_A \sqrt{f_{H_2}}\right)\right]}{\left(1 + K_{CO} f_{CO} + K_{CO_2} f_{CO_2}\right)\left[\sqrt{f_{H_2}} + \left(K_{H_2O} / \sqrt{K_H}\right) f_{H_2O}\right]} \quad (8)$$

$$r_{CO,B2} = r_{H_2O,B2} = k_B \frac{K_{CO_2}\left[f_{CO_2} f_{H_2} - f_{H_2O} f_{CO} / K_B\right]}{\left(1 + K_{CO} f_{CO} + K_{CO_2} f_{CO_2}\right)\left[\sqrt{f_{H_2}} + \left(K_{H_2O} / \sqrt{K_H}\right) f_{H_2O}\right]} \quad (9)$$

$$r_{CH_3OH,C3} = r_{H_2O,C3} = k_C \frac{K_{CO_2}\left[f_{CO_2} {f_{H_2}}^{3/2} - f_{H_2O} f_{CH_3OH} \Big/ \left({f_{H_2}}^{3/2} K_C\right)\right]}{\left(1 + K_{CO} f_{CO} + K_{CO_2} f_{CO_2}\right)\left[\sqrt{f_{H_2}} + \left(K_{H_2O} / \sqrt{K_H}\right) f_{H_2O}\right]} \quad (10)$$

4. Results and discussion

4.1. Process design and simulation

The methanol production process presented in this work (Fig. 1) takes into account the raw materials conditioning, hydrogenation reaction, recycling of unreacted reagents and product separation. Wet hydrogen (11% wt of water) is fed to the unit at 1.1 bar from a water electrolyzer and compressed up to 65 bar in a five stages compressor (H2COMP) with intercooling at 55 °C and interstage knock-out (KO) drums. Air is used as cooling agent for interstage cooling to minimize cooling water consumption in the plant. If cooling water is used as cold utility and the interstage temperature is reduced even further, the compression power can be decreased more. In this work, it has been considered that the plant is located in a place where the maximum ambient temperature is 45 °C and that the temperature difference between the air used in the air coolers of the plant and the process fluid temperature is at least 10 °C. The selection between cooling water or air and thus, the interstage temperature, will depend on the availability of cooling water and the plant location. Five compression stages are the minimum number of stages that avoids exceeding an interstage or discharge temperature of 176 °C, considered as the maximum allowed

Table 1
Kinetic factor for reactions A, B and C (based on data from An et al. (2019)) – the units used are [Pa] for fugacity and [mol/$g_{catalyst}$ s] = [kmol/$kg_{catalyst}$ s] for reaction rate.

Reaction	k	n	Ea [J/mol K]
A	4.0638×10^{-6} [kmol/kgcat s Pa]	0	11,695
B	9.0421×10^{8} [kmol/kgcat s $Pa^{1/2}$]	0	112,860
C	1.5188×10^{-33} [kmol/kgcat s Pa]	0	266,010

Table 2
Constants for driving force (from An et al. (2019)) using the format for Aspen Plus.

	K1		K2	
Reaction	A	B	A	B
A	−23.20	14,225	28.895	2,385
B	−22.48	9,777	−28.12	15,062
C	−22.48	9,777	23.974	3,222

Table 3
Ki factors for adsorption term (terms 2, 3, 5 from An et al. (2019); rest is explicitly derived by calculation).

Term	Expression	$A_i = \ln(a_i)$	$B_i = b_i/R$	$\prod c_j^{\nu_j}$
1	1	0	0	$\sqrt{f_{H_2}}$
2	$\frac{K_{H_2O}}{\sqrt{K_H}}$	−26.1568	13,842	f_{H_2O}
3	K_{CO}	−23.2006	14,225	$f_{CO}\sqrt{f_{H_2}}$
4	$\frac{K_{CO}K_{H_2O}}{\sqrt{K_H}}$	−49.3574	28,067	$f_{CO}f_{H_2O}$
5	K_{CO_2}	−22.4827	9777	$f_{CO_2}\sqrt{f_{H_2}}$
6	$\frac{K_{CO_2}K_{H_2O}}{\sqrt{K_H}}$	−48.6395	23,619	$f_{CO_2}f_{H_2O}$

temperature (MAT) for the compressor (Giampaolo, 2010). The pressure ratio within the different stages was adjusted to have the same one in all the stages. This leads to the most efficient design in terms of compressor load and power consumption. During the compression and refrigeration process, part of the water of the hydrogen feed stream condenses and it is recovered in the interstage KO drums.

Similarly, CO_2 is compressed from 1.1 bar to 65 bar in a 4 stages compressor (CO2COMP) with intercooling to 55 °C and interstage KO drums. In this case, 4 compressor stages were sufficient to not exceed the MAT of 176 °C (Giampaolo, 2010). A feed pressure of 1.1 bar is selected considering that the methanol production unit is located downstream of the regenerator of a CO_2 amine capture unit that operates near the atmospheric pressure (Li et al., 2013). In this compressor, around 65% of the methanol recycled from the DWC overhead stream condenses and is sent back to the DWC since the presence of methanol in the hydrogenation reaction would reduce the equilibrium conversion. As both hydrogen and CO_2 compressors are driven by green electricity, if it is not possible to ensure a constant supply of green electricity to the plant, an additional and more stable backup power source would be also needed. The compressed CO_2 stream is mixed with the recycling stream coming from the recycling compressor (RCOMP) and containing the unreacted reagents and with the hydrogen stream coming from the hydrogen makeup compressor (H2COMP). The resulting stream is heated first in the feed-effluent heat exchanger (FEHE) – at the same time cooling the reaction products – and then in the steam heater (HEATER) to adjust the temperature to 220 °C using the steam generated in the reactor. For the startup of the plant, an external heat supply source is needed to reach a reactor feed stream temperature close to the normal operating temperature (220 °C). Once this temperature is reached, the process becomes thermally self-sufficient. Then, the reagents enter the reactor where they are converted into products. The FEHE cold side outlet temperature is set at 177 °C. In this way, all the heat produced in the hydrogenation reactor is useable in the HEATER and the LMTD of the FEHE is maximized. In the case of the HEATER, an outlet temperature of 220 °C is needed to maintain a minimum LMTD of 15 °C with respect to the saturation temperature of the high pressure steam produced in the hydrogenation reactor (235 °C).

The catalytic hydrogenation reactor operates isothermally at 250 °C using high pressure water as coolant to absorb the heat of reaction and generate high pressure steam that is used in the HEATER. The PFR is a multitubular reactor consisting of 670 tubes with a length of 12m and a diameter of 6 cm, charged with 865 kg of Cu/Zn/Al/Zr catalyst and having a bed voidage of 0.98. A reaction temperature of 250 °C and 865 kg of catalyst are selected in line with the data from Kiss et al. (2016). While lower reaction temperatures mean higher catalyst needs to reach the equilibrium conversion, at temperatures higher than 250 °C the process is equilibrium limited and the equilibrium conversion decreases. The amount of catalyst selected ensures that the reaction reaches the equilibrium conversion.

The reaction products at 250 °C are used as heating source in the FEHE, in the DWC reboiler (REBOILER), and in the vaporizer (VAP). Although the process is thermally self-sufficient, as shown in the grand

Table 4
Comparison of experimental data from An et al. (2019) and Park et al. (2015) with the results of the Aspen Plus calculations.

Space velocity = 6000 mL/(gcat·h)		Feed Composition (mol/mol)				Conversion % CO2	
Pressure (bar)	Temperature (K)	CO	CO2	H2	Ar	Experimental data (a)	Aspen Plus Calculations
50	483	0.00	0.25	0.75	0.00	17.00	12.44
50	503	0.00	0.25	0.75	0.00	22.50	19.57
50	523	0.00	0.25	0.75	0.00	25.50	23.98
50	543	0.00	0.25	0.75	0.00	25.00	24.04
T = 523K		Feed Composition (mol/mol)				Conversion % CO2	
Pressure (bar)	Space velocity mL/(gcat·h)	CO	CO2	H2	Ar	Experimental data (a)	Aspen Plus Calculations
50	1000	0.00	0.25	0.75	0.00	26.20	24.28
50	2000	0.00	0.25	0.75	0.00	26.00	24.28
50	4000	0.00	0.25	0.75	0.00	25.60	24.21
50	6000	0.00	0.25	0.75	0.00	25.00	23.98
50	8000	0.00	0.25	0.75	0.00	24.30	23.62
50	10,000	0.00	0.25	0.75	0.00	23.00	23.21
Space velocity = 8000 mL/(gcat·h)		Feed Composition (mol/mol)				Conversion % CO2	
Pressure (bar)	Temperature (K)	CO	CO2	H2	Ar	Experimental data (b)	Aspen Plus Calculations
60	523	0.00	0.24	0.72	0.04	26.21	24.74
60	523	0.00	0.17	0.80	0.03	34.23	33.00
60	523	0.00	0.12	0.86	0.02	45.15	42.03
70	523	0.00	0.24	0.72	0.04	28.70	26.10
70	523	0.00	0.17	0.80	0.03	35.98	35.06
70	523	0.00	0.12	0.86	0.02	48.44	44.84
70	543	0.00	0.24	0.72	0.04	26.46	26.50

a) Experimental data from An et al. (Bowker, 2019).
b) Experimental data from Park et al. (Bowker, 2019).

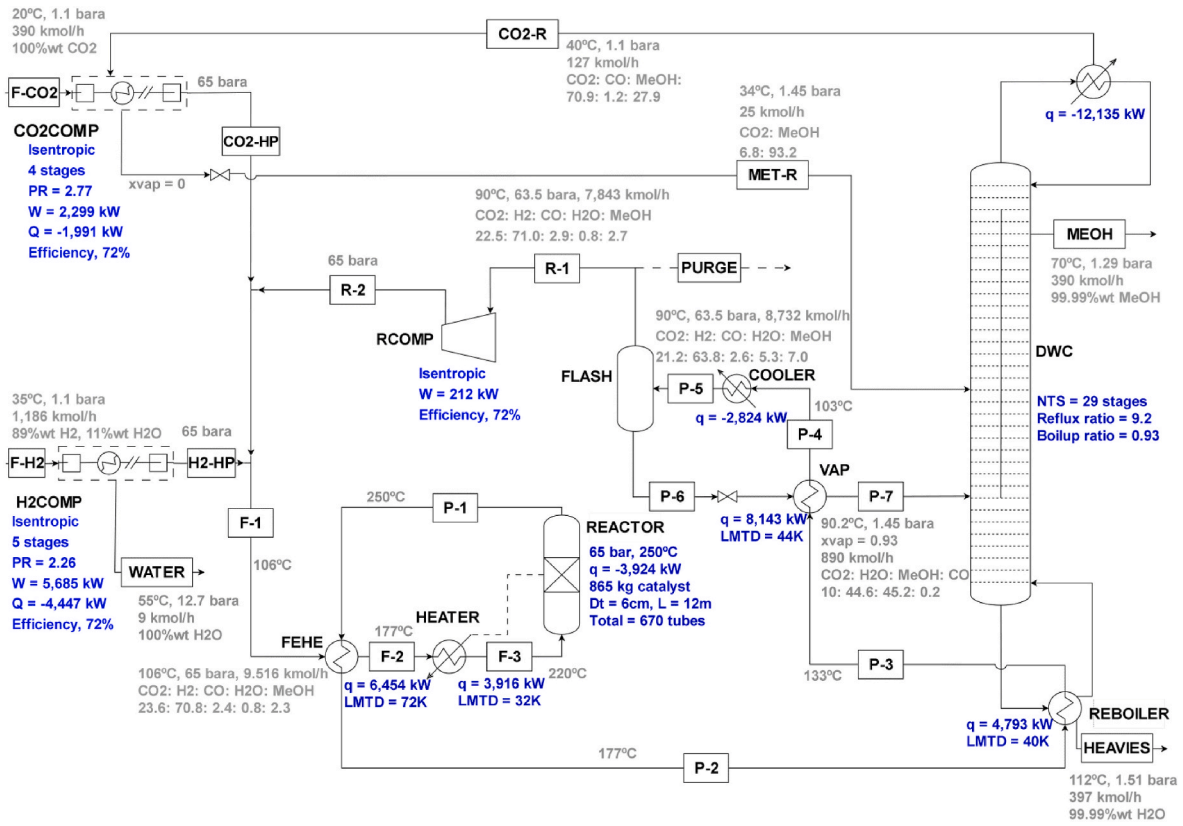

Fig. 1. Process flow diagram of a thermally self-sufficient process for methanol production by CO_2 hydrogenation.

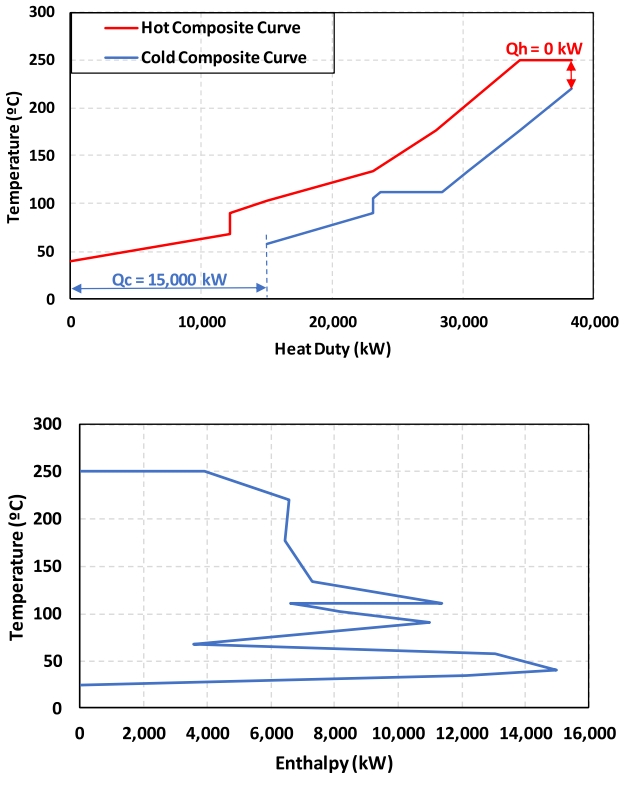

Fig. 2. Hot and cold composite curves (upper graph) and Grand Composite Curve (lower graph) of a thermally self-sufficient process for methanol production by CO_2 hydrogenation.

composite curve provided in Fig. 2, a minimum logarithm mean temperature difference (LMTD) must exist in the heat exchangers. Otherwise, the heat exchanger dimensions will increase beyond the limits of a technically and economically feasible design. This is especially relevant in those heat exchangers in which either the hot side and/or the cold side is a gas (lower heat transfer coefficient). In the proposed process, the HEATER has the lowest LMTD (32K). However, this heat exchanger operates with steam condensation on the hot side (high heat transfer coefficient). In the case of the FEHE, the LMTD is 72K, sufficiently high to compensate for the lower overall heat transfer coefficient (gas-gas exchanger). Finally, in the case of the DWC reboiler and the vaporizer (LMTDs higher than 40K), since part of the vapor stream condenses inside the heat exchangers, higher heat transfer coefficients are expected.

After being cooled in the vaporizer, the reaction products are further cooled down to 90 °C in a last trim cooler (COOLER) and the resulting vapor and liquid phases are separated in a flash (FLASH). The unreacted hydrogen, a cost driver of the process, is recovered in the FLASH vapor stream. This cooler also works with air to reduce the cooling water usage in the plant. Using a flash operating temperature of 90 °C is optimal to minimize the power requirements in compressors. Lower operating temperatures lead to higher recycles to the CO_2 compressor, while higher temperatures increase the recycling compressor power. The overhead gases of the flash are recycled to the reactor through the recycling compressor (RCOMP), while the liquid phase is expanded in a valve up to the operating pressure of the DWC and passes through the vaporizer (VAP) being vaporized up to a 0.93 M vapor fraction. As explained later, this molar vaporization fraction minimizes the heat transfer area required in the vaporizer and reboiler. Then, this stream is fed to the prefractionator side of the DWC. As there is no valve in the reaction-separation-recyle loop, the pressure increase in the recycling compressor is minimized since it only corresponds with the pressure drop across the reaction-separation loop. Although a higher operating

pressure in the flash means a higher solubility of CO_2 leading to a higher duty in the DWC reboiler and a higher recycle of CO_2 at the top of the DWC, the thermal self-sufficiency of the process and the reduction of power consumption in the recycle compressor compensates the increase of power in the CO_2 makeup compressor and makes it worthy to operate without reducing the pressure (only the pressure drop) in the reaction-separation-recycle loop.

Finally, a DWC is used to recover the lights as top product, high purity methanol product as side-stream, and water by-product as bottom stream. The DWC is a 29 trays column that operates at 1.3 bar to have sufficient pressure difference to recycle the overhead gas to the CO_2 makeup compressor (CO2COMP). The reactor liquid product (stream P-7) is fed at the bottom of the prefractionator section of the column (stage 23), whereas the methanol-rich stream coming from the interstage KO drums of the CO_2 compressor is fed at stage 14. There are two stages over the dividing wall and 6 stages under it. Using 29 stages minimizes the overall costs of the column. The feed streams trays are selected as those whose liquid compositions match the composition of the feed streams. The DWC partial condenser operates at 40 °C using cooling water as cold utility. The selection of the operating pressure and condenser temperature determines the amount of methanol that is recycled to the CO_2 compressor. The higher the column operating pressure and the lower the condensation temperature, the lower the methanol recycling. In this work, an operating pressure close to the atmospheric pressure has been selected to minimize the capital costs of the column. In the case of the condenser temperature, 40 °C is considered the minimum temperature that can be reached using cooling water in the plant. If the plant is located in a country in which it is possible to cool down a process stream to 40 °C using air, the plant will only need electricity and air as cold utility and no cooling water would be consumed. If the condensation temperature can be decreased below 40 °C, the methanol recycling, and consequently the CO_2 compressor power, will be reduced. The methanol product stream (>99.99% mass) is taken from the product side of the wall (at stage 4) as the methanol composition is highest on this tray. On the other hand, water is recovered at the bottom of the column (>99.99% mass). As there is no purge and the separation is very efficient in the distillation column, the methanol yield and methanol recovery are practically 100%. If any inert or undesirable compound is present in the feed streams, a purge stream is required at the vapor overhead line of the flash. The complete heat and material balance of the proposed process is provided in Table 5, while the equipment sizing and main design parameters are provided in the *Supplementary Information* file.

4.2. Sensitivity analysis

This section of the work is aimed at describing how the different process parameters influence the overall performance of the newly proposed process.

4.2.1. Reactor technology selection

An isothermal reactor operated at a reaction temperature of 250 °C has been selected based on the previous work of Kiss et al. (2012, 2016) as this reaction temperature provides a trade-off between the amount of catalyst needed and the equilibrium conversion reached. However, two more reactor configurations have been also analyzed.

- An adiabatic reactor, in which the heat generation in the reactor is reduced as the reaction temperature increases and the equilibrium conversion decreases. Thus, if the process needs to be thermally self-sufficient, the operating pressure in the reactor has to be increased with respect to the isothermal operating case to compensate for the decrease in the equilibrium conversion. Moreover, as there is no heat transfer in the reactor, no steam can be generated and the FEHE exchanger needs to account for all the temperature increase of the

Table 5
Mass and energy balance of the proposed process.

	F–CO_2	CO_2-HP	MET-R	F–H_2	H_2-HP	WATER	F-1	F-2	F-3	P-1	P-2
Temperature (°C)	25.0	163.5	29.9	35.0	175.0	55.3	105.6	177.0	220.0	250.0	176.8
Pressure (bar)	1.1	65.0	1.5	1.1	65.0	12.7	65.0	64.9	64.7	64.1	64.0
Vapor frac (mol/mol)	1	1	0.045	1	1	0	1	1	1	1	1
Mole flow (kmol/h)	390.0	492.3	24.9	1186.1	1177.1	9.1	9512.7	9512.7	9512.7	8732.7	8732.7
Mass flow (kg/h)	17,164	21,496	819	2650	2487	163	127,146	127,146	127,146	127,146	127,146
Volume flow (cum/h)	8736	250	20	27,635	688	0	4579	5517	6081	5933	5058
Enthalpy (gcal/h)	−36.72	−45.20	−1.48	−0.85	0.83	−0.62	−226.94	−221.38	−218.01	−221.39	−226.95
Mass frac CO_2	1.0000	0.9796	0.0910	0.0000	0.0000	0.0000	0.7761	0.7761	0.7761	0.6411	0.6411
Mass frac H_2	0.0000	0.0000	0.0000	0.8900	0.9485	0.0000	0.1069	0.1069	0.1069	0.0884	0.0884
Mass frac CO	0.0000	0.0020	0.0000	0.0000	0.0000	0.0000	0.0504	0.0504	0.0504	0.0504	0.0504
Mass frac METHANOL	0.0000	0.0183	0.9090	0.0000	0.0000	0.0000	0.0561	0.0561	0.0561	0.1543	0.1543
Mass frac WATER	0.0000	0.0000	0.0000	0.1100	0.0515	1.0000	0.0105	0.0105	0.0105	0.0658	0.0658
Mole frac CO_2	1.0000	0.9719	0.0679	0.0000	0.0000	0.0000	0.2357	0.2357	0.2357	0.2121	0.2121
Mole frac H_2	0.0000	0.0000	0.0000	0.9864	0.9940	0.0000	0.7091	0.7091	0.7091	0.6384	0.6384
Mole frac CO	0.0000	0.0032	0.0000	0.0000	0.0000	0.0000	0.0241	0.0241	0.0241	0.0262	0.0262
Mole frac METHANOL	0.0000	0.0250	0.9320	0.0000	0.0000	0.0000	0.0234	0.0234	0.0234	0.0701	0.0701
Mole frac WATER	0.0000	0.0000	0.0000	0.0136	0.0060	1.0000	0.0078	0.0078	0.0078	0.0531	0.0531
	P-3	P-4	P-5	P-6	P-7	PURGE	R-1	R-2	CO_2-R	MEOH	HEAVIES
Temperature (°C)	133.4	102.7	89.8	89.8	90.2	89.8	89.8	92.9	40.0	70.5	111.5
Pressure (bar)	63.8	63.7	63.5	63.5	1.5	63.5	63.5	65.0	1.3	1.3	1.5
Vapor frac (mol/mol)	0.988	0.919	0.898	0	0.930	1	1	1	1	0	0
Mole flow (kmol/h)	8732.7	8732.7	8732.7	889.4	889.4	0	7843.3	7843.3	127.3	390.0	397.1
Mass flow (kg/h)	127,146	127,146	127,146	23,982	23,982	0	103,163	103,164	5151	12,497	7154
Volume flow (cum/h)	4488	3919	3721	30	16,960	0	3691	3639	2596	17	8
Enthalpy (gcal/h)	−231.12	−238.13	−240.52	−57.77	−50.75	0	−182.75	−182.57	−10.22	−21.82	−26.51
Mass frac CO_2	0.6412	0.6412	0.6411	0.1624	0.1624	0.0000	0.7524	0.7524	0.7705	0.0000	0.0000
Mass frac H_2	0.0884	0.0884	0.0884	0.0000	0.0000	0.0000	0.1089	0.1089	0.0000	0.0000	0.0000
Mass frac CO	0.0504	0.0504	0.0504	0.0018	0.0018	0.0000	0.0617	0.0617	0.0084	0.0000	0.0000
Mass frac METHANOL	0.1543	0.1543	0.1543	0.5375	0.5375	0.0000	0.0653	0.0653	0.2211	1.0000	0.0000
Mass frac WATER	0.0657	0.0657	0.0658	0.2983	0.2983	0.0000	0.0117	0.0117	0.0000	0.0000	1.0000
Mole frac CO_2	0.2122	0.2122	0.2121	0.0995	0.0995	0.0000	0.2249	0.2249	0.7086	0.0000	0.0000
Mole frac H_2	0.6384	0.6384	0.6384	0.0000	0.0000	0.0000	0.7108	0.7108	0.0000	0.0000	0.0000
Mole frac CO	0.0262	0.0262	0.0262	0.0017	0.0017	0.0000	0.0290	0.0290	0.0122	0.0000	0.0000
Mole frac METHANOL	0.0701	0.0701	0.0701	0.4523	0.4523	0.0000	0.0268	0.0268	0.2792	1.0000	0.0000
Mole frac WATER	0.0531	0.0531	0.0531	0.4465	0.4465	0.0000	0.0085	0.0085	0.0000	0.0000	1.0000

reagents up to the reactor inlet temperature. As the FEHE is a gas-gas heat exchanger with a low heat transfer coefficient, any reduction in the LMTD drastically increases the total required area. Thus, although the reactor may be simpler than in the isothermal operating case and the HEATER located before the reactor is not required, more power is needed in the compressors and the heat exchangers are larger and operate at a higher pressure.

- Reactor with intercooling, which is something in between isothermal and adiabatic alternatives. Although the reactor is adiabatic, the intercooling reduces the reaction temperature allowing increasing the equilibrium conversion with respect to the adiabatic case and also recovering some heat as steam. The main drawback of this alternative is the higher investment cost expected for the reactor.

In this work, an isothermal reactor of 670 tubes (12m length and 6 cm diameter) with a catalyst load of 865 kg has been selected as the best option, since the investment cost is lower than in the case of the adiabatic reactor with intercooling and the operating pressure in the reactor and heat transfer areas required in the heat exchangers are lower than in the case of the adiabatic reactor. At the industrial level, several companies (Casale, 2023; Topsoe, 2023; Linde, 2023) can provide isothermal reactors for methanol synthesis, with similar performance. Casale IMC technology (*Isothermal Methanol Converter*) is based on the use of exchanger plates in place of tubes. In particular, the IMC steam rising reactor is a one-bed isothermal converter that circulates boiler feed water and produces steam. In the case of Topsoe technology, the methanol synthesis process relies on an ultra-efficient tubular boiling water reactor (BWR) in which the catalyst is loaded into tubes that are cooled from the shell side by boiler feed water, achieving an almost isothermal reaction path. Linde uses a fixed bed isothermal reactor cooled by coiled pipes, in which the reaction temperature is maintained by steam production in the pipe interiors.

4.2.2. *Operating pressure of the hydrogenation reactor*

Increasing the operating pressure in the reactor increases the equilibrium conversion and heat generation in the reactor. A higher operating pressure means also more condensation after the COOLER and a lower recycle to the reactor, which also increases the equilibrium conversion and the heat generation because of the lower amount of methanol and water recycled to the reactor. A higher generation of heat in the reactor means that more steam can be produced and used in the HEATER, which has a higher heat transfer coefficient than the FEHE, as it is based on steam condensation. Thus, the LMTDs of the FEHE, VAPORIZER and REBOILER increase and their areas decrease. Moreover, when operating at a higher pressure, the recycle flowrate and consequently the duties and areas of the FEHE, the VAPORIZER and the REBOILER are lower. In this work, it has been considered that all the heat released in the reactor is used to produce the steam consumed in the steam heater. As the duty required in the steam heater and the duty released in the reactor are practically the same, no extra steam is needed. If there is any inefficiency in the production or consumption of steam, the FEHE cold side outlet temperature can be increased to reduce the duty required in the steam heater, although this will mean an increase in the FEHE and DWC reboiler and prevaporizer areas. Conversely, when operating at a higher pressure, more power is required in the CO_2 and hydrogen compressors. Fig. 3 shows the effect of the reactor operating pressure on the total heat transfer area required in the unit and on the total power consumption in the compressors of the plant. While there is an exponential decrease in the heat transfer area requirements when increasing the pressure, the increase in the required compressor power is linear.

Regarding the reactor volume, operating at a higher pressure means that the gas density is higher, the gas velocity is lower and that a higher mass of gas can flow through each tube of the reactor while maintaining the same space velocity. Moreover, a higher operating pressure means a smaller recycle and therefore less flow of gas to the reactor and a lower number of tubes. Fig. 4 shows the evolution of the number of tubes required in the reactor (to maintain the same space velocity) with the operating pressure of the reactor.

Figs. 3 and 4 prove that increasing the operating pressure of the reactor decreases both the heat transfer area required and the reactor volume. However, increasing the operating pressure means also an increase in the thickness of the equipment and therefore a higher cost. To determine the optimal operating pressure of the plant, Aspen Plus Economic Analyzer was used to obtain the total equipment cost at different operating pressures. As shown in Fig. 5, the total equipment cost is minimized when operating the reactor at 65 bar. While the cost of the CO_2 and hydrogen compressors increases with the pressure, the cost of the recycling compressor is minimized at 65 bar (when operating at lower pressure, the flowrate increases). The same behavior is observed for the cost of the flash vessel. In the case of the reactor and the DWC, the equipment cost increases with the pressure. Finally, for the heat exchangers, the equipment costs decrease with the pressure because of the increase in the LMTD and the reduction of the required area. At lower operating pressures the pieces of equipment are larger and more expensive and at higher operating pressures, although the heat exchangers and the recycle compressors are smaller, the thickness increase results in more expensive equipment. Finally, considering that the compressors' total power increases with the operating pressure, a Total Annualized Cost (TAC) vs Reactor Operating Pressure curve is presented in Fig. 6. As can be seen from Fig. 6, the optimum operating pressure is also around 65 bar. This graph has been prepared considering a payback time of 8.5 years to annualize the Total Investment Costs and a Lang's factor of 5. The TAC is mainly influenced by the operating costs and especially, by the price of the raw materials. An electricity price of 0.05 €/kWh has been used to calculate the utilities costs. While a higher

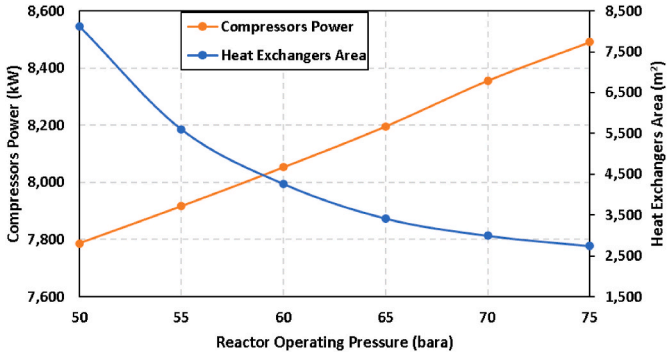

Fig. 3. Compressors power and heat exchangers area at various reactor pressures.

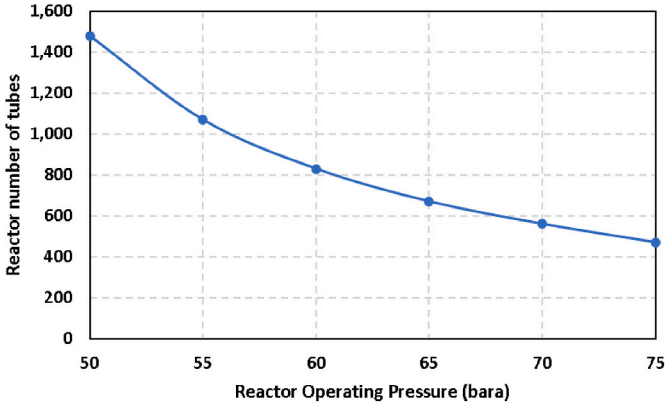

Fig. 4. Number of tubes in the hydrogenation reactor required at various reactor pressures.

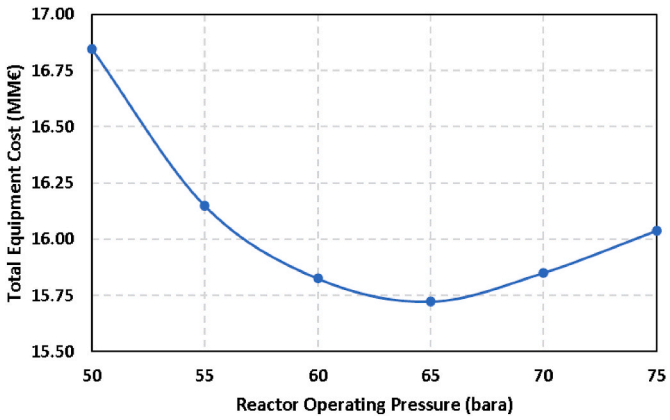

Fig. 5. Total equipment cost at various reactor pressures.

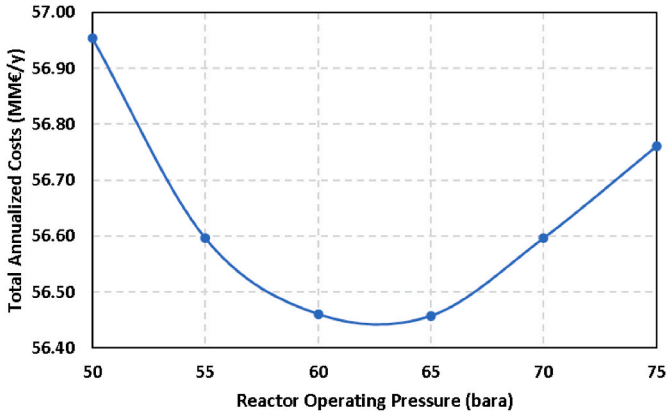

Fig. 6. Total annualized costs (TAC) at various reactor pressures.

electricity price will move the optimum operating pressure slightly closer to 60 bar to mitigate the increase in the electricity price with lower power consumption in the compressors, a lower electricity price will move the optimum operating pressure close to 65 bar.

4.2.3. *Post-reaction heat recovery*

The reaction products are first cooled down in the FEHE, increasing the temperature of the reactants to 177 °C. The FEHE cold side outlet temperature determines whether all the steam produced in the reactor is consumed in HEATER or if there is a surplus of steam. Operating at temperatures above 177 °C results in a steam surplus but also in a reduction of the FEHE LMTD, while operating at 177 °C implies maximization of the FEHE LMTD and that all the steam produced in the reactor is consumed in HEATER. A FEHE cold side outlet temperature lower than 177 °C means that the heat produced in the reactor is insufficient to cover the HEATER duty and therefore, the requirement of an external heat source to heat the reactants to 220 °C (reactor inlet temperature). As higher operating pressures in the reactor result in more heat generation, the FEHE outlet temperature can be gradually decreased (increasing the FEHE LMTD and reducing its area) as the operating pressure in the reactor increases.

Regarding the vaporizer and reboiler duties, the duty required in the reboiler of the DWC is linked to the duty that is supplied in the vaporizer. While increasing the vaporization of the DWC feed stream implies a reduction in the duty of the column reboiler, when the vaporization of the feed stream is reduced, the reboiler duty increases. Although the process is thermally self-sufficient and does not rely on the consumption of external fuels, depending on the feed stream vaporization there is a variation in the reboiler and vaporizer duties and therefore in their heat transfer areas. For this reason, a sensitivity analysis was performed to

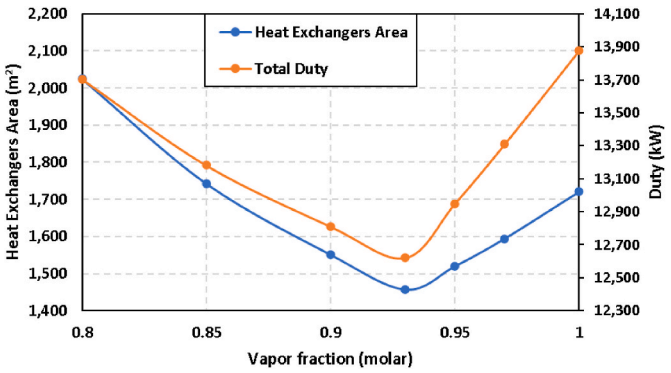

Fig. 7. Vaporizer and reboiler total area and duty vs vaporizer outlet molar vapor fraction.

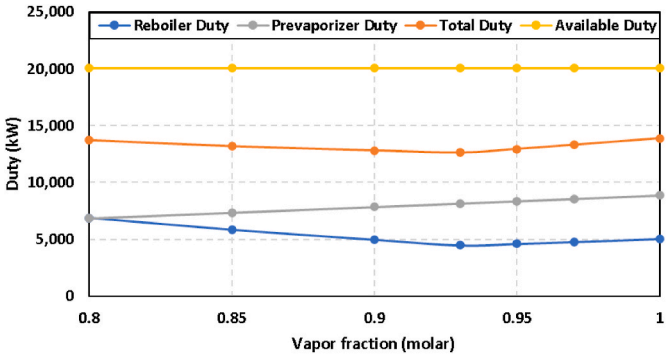

Fig. 8. Reboiler, vaporizer total, and available duty vs vaporizer outlet molar vapor fraction.

obtain the optimal feed stream vaporization, understood as that vaporization that minimizes the total heat transfer area and total duty required both in the vaporizer and the column reboiler. As shown in Fig. 7, the total heat transfer area and the total required duty (vaporizer + reboiler) are minimized when the DWC feed stream vaporization is fixed at 0.93. Thus, this vaporization value was selected in the process. Moreover, in Fig. 8 can be seen that a vaporization of 0.93 also minimizes the column reboiler duty and that the total required duty (around 14 MW for all the vaporizations) remains below the available duty (20 MW).

4.2.4. *Flash separation temperature*

The selection of the COOLER outlet temperature affects the heat generation in the reactor and the total power required in the compressors. Decreasing the cooler outlet temperature means that less methanol and water are recycled back to the reactor and therefore, a higher equilibrium conversion and a higher heat generation in the hydrogenation reactor. Decreasing the cooler outlet temperature also means lower power requirements in the recycling compressor (as there is more condensation of products), but an increase in the CO_2 compressor power (as more CO_2 is solubilized in the liquid stream of the flash and recycled to the CO_2 compressor). On the other hand, increasing the operating temperature over 90 °C results in a fast increase of the required area in the heat exchangers of the plant and therefore of the equipment cost. In this work, the cooler outlet temperature was adjusted to 90 °C as this temperature minimizes the Total Annualized Costs (TAC) of the plant, as is shown in Fig. 9. For the calculation of the TAC, a Lang's factor of 5 and an electricity price of 0.05 €/kWh have been considered. While higher electricity prices will move the optimum cooler outlet temperature close to 95 °C, for lower electricity prices, the optimum cooler outlet temperature will be closer to 85 °C. In this work, the cooler outlet temperature was adjusted to 90 °C as this temperature minimizes the overall

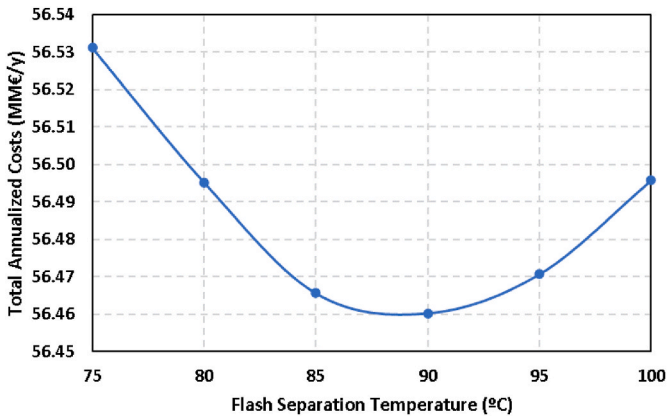

Fig. 9. Total annualized costs (TAC) at various flash separation temperatures.

power consumption in the plant.

4.2.5. Dividing wall column design

The last step in the design of the process was the optimization of the DWC. The DWC is divided into three sections: upper common section (trays above the wall), middle divided section (trays along the dividing-wall) and lower common section (trays below the wall). The DWC is simulated using four rigorous distillation RADFRAC columns located in a subflowsheet of the simulation. More details on the DWC simulation can be found in the *Supplementary Information* file. The main objective was to optimize the number of trays in all sections of the column and the liquid split ratio, since the boilup and reflux ratio are adjusted to ensure minimum methanol and water purities of 99.99% mass. Regarding the feed streams optimum feed stages, stream P7 (outlet of the vaporizer) was fed at the last tray of the middle left section of the column, while the methanol recycle stream (MET-R) was also fed at tray 14, as the composition of the liquid of this tray is similar to the composition of this stream.

For the upper section, two trays are sufficient as there is no change in the liquid and vapor compositions when more trays are used. The optimization of the number of trays in the middle section was done using the N-Q plot (number of trays vs reboiler duty) and the N × (RR+1) vs N plot (number of trays multiplied by reflux ratio plus 1 vs number of trays) fixing as design specifications the methanol composition in the side stream and the water composition in the bottoms stream. The latter plot combines both the capital cost of the column, as it includes the number of trays (N), with the operating costs, as it accounts for the reflux ratio (RR+1). Fig. 10 shows that it is not worth considering more than 25 trays in this section of the column, as there is no decrease in the reboiler duty, while the N × (RR+1) vs N curve confirms that the optimum number of trays for this section is 21 as it minimizes the total costs of the column. The side stream rate flowrate is fixed at 390 kmol/h, as this is the maximum methanol production (100% yield) that can be obtained in the process. The methanol stream is taken from the second tray of the right side of the divided wall section, as this tray yields the highest methanol composition of all the DWC. For the lower section, Fig. 11 shows that the reboiler duty is not further reduced when more than 7 trays are used, while the N × (RR+1) vs N curve proves that the optimum number of trays for this section is 6. Thus, by adding the optimum number of trays of each section, a total optimum number of trays equal to 29 is obtained for the whole DWC.

Finally, the last part of the analysis is dedicated to optimizing the liquid split ratio in the column (liquid split ratio and vapor split ratio are considered to be equal in the column). To measure the influence of this parameter, the variation of the reboiler duty with the liquid split ratio was depicted in a new graph. Fig. 12 shows that the minimum reboiler duty is obtained when the liquid split ratio is fixed at 0.55 (towards the prefractionator side of the DWC). The reboiler duty required in this

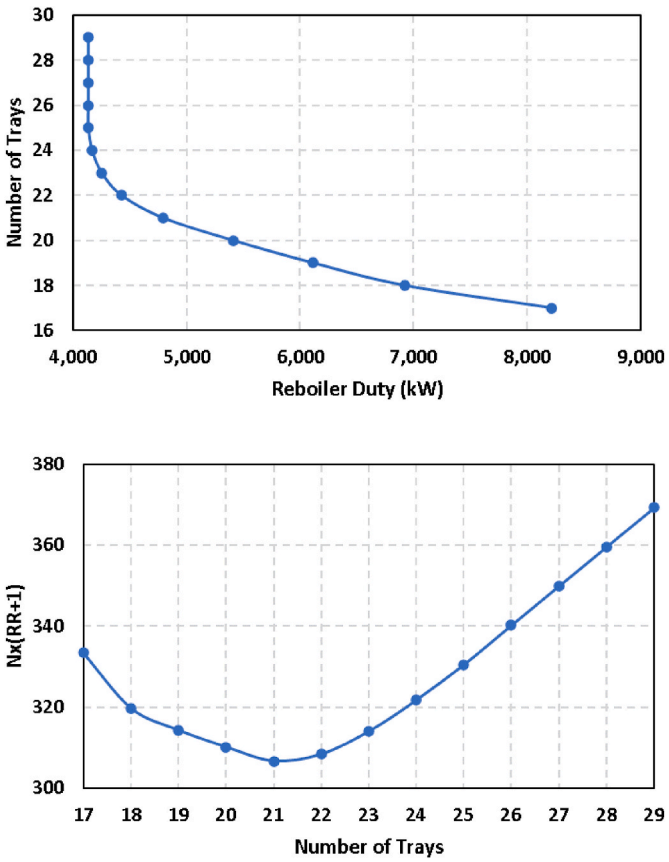

Fig. 10. Number of trays vs reboiler duty for the middle section of the DWC (top). Variation of $N \times (RR+1)$ with number of trays for the middle section of the DWC (bottom).

column (4793 kW) is 37% lower than the duty required in the reboiler of a conventional methanol distillation column with the same methanol production capacity (100 kton/y), such as the one shown in Kiss et al. (2016) work.

Regarding the vapor split ratio, in this work, the vapor split ratio is fixed to the optimized liquid split ratio value resulting in an easier design of the DWC. The temperature and composition profiles along the DWC are provided in Figs. 13 and 14.

4.3. Key parameters and consumption figures

Table 6 compares the key parameters and consumption figures of this process with the results from previous works. Although a direct comparison with the results of all the previous published works on methanol production by CO_2 hydrogenation is not straightforward due to the lack of data in some works, the authors have compiled the best of those which allowed a direct comparison with Kiss et al. (2016) and other works.

Table 6 demonstrates that this work presents a competitive process alternative that improves the results obtained by Kiss et al. (2016) and by the rest of the most representative works shown in the table. The process is thermally self-sufficient, consumes less electricity per ton of methanol, the catalyst load in the reactor per ton of methanol produced is the lowest one and, although it uses a DWC that is more expensive than a conventional distillation column, the number of trays is lower than in the rest of the reported cases and no stripper is needed.

Pérez-Fortes et al. (2016) presented a process based on the use of two steam turbines to generate power consumed in the plant. The process was not thermally self-sufficient and required a distillation tower of 57 stages (28 stages more than in the DWC of this work), and 44.5 tons of catalyst in the reactor (more than ten times the amount of catalyst

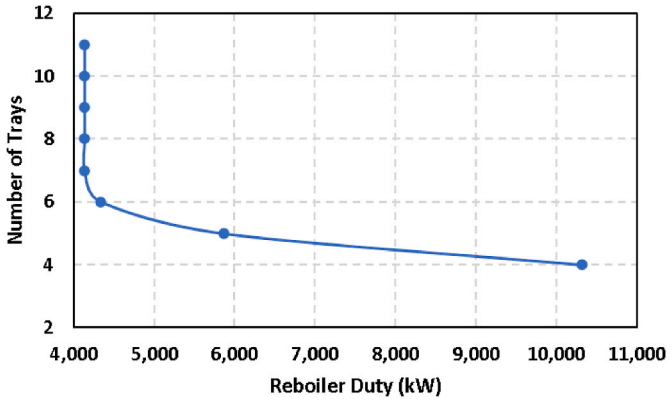

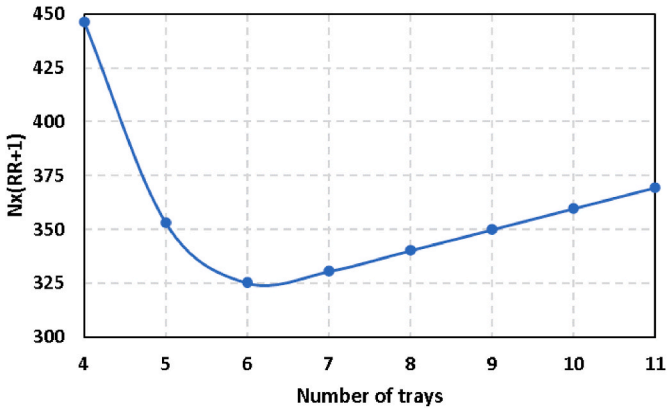

Fig. 11. Number of trays vs reboiler duty for the lower section of the DWC (top). Variation of $N \times (RR+1)$ with the number of trays for the lower section of the DWC (bottom).

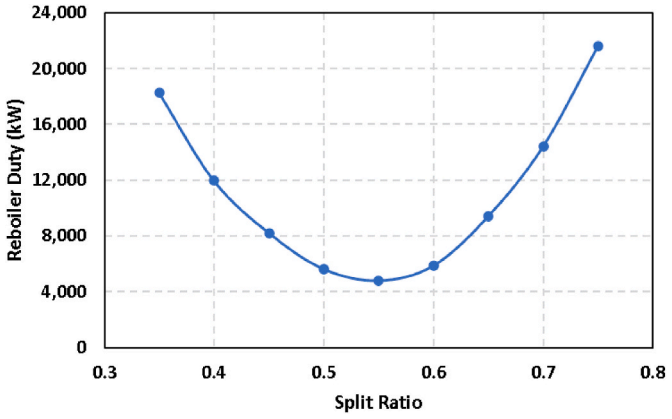

Fig. 12. Reboiler duty vs liquid split ratio for the DWC.

required in this work per ton of methanol). Moreover, the methanol yield is lower than 95%, meaning that part of the CO_2 fed to the unit is not converted into methanol.

Meunier et al. (2020) presented a thermally self-sufficient process based on an adiabatic reactor that operates at 80 bar and whose outlet temperature is equal to 314 °C. The process needed 156 tons of catalyst in the reactor (more than thirty times the amount of catalyst required in this work per ton of methanol), one heat exchanger more than in the process presented in this work, the methanol purity was lower (99.10% wt) and the overall methanol yield was lower than 95%.

GhasemiKafrudi et al. (2022) proposed the use of a new catalyst instead of the one used by Kiss et al. in (2016). This allowed for reducing

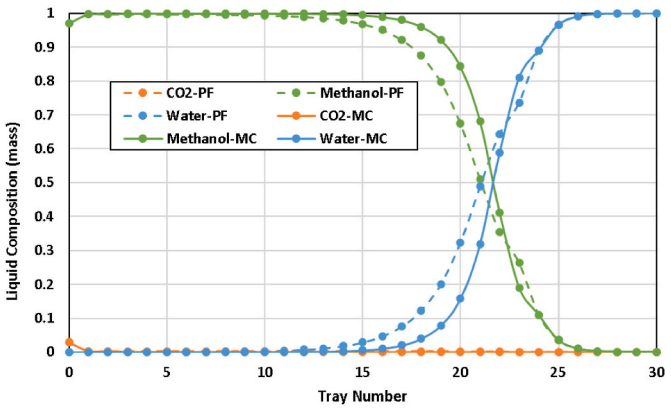

Fig. 13. Composition profiles along the DWC.

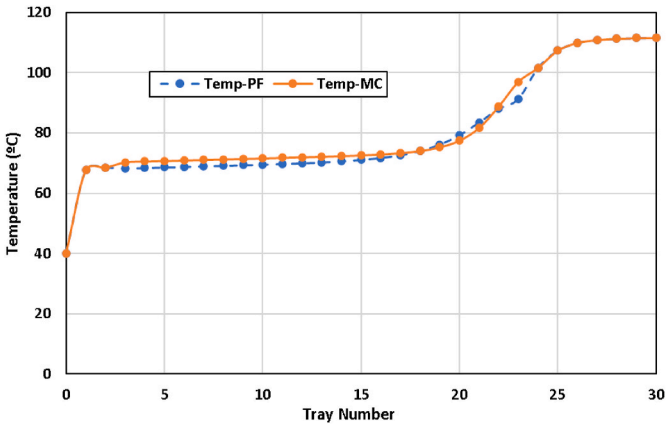

Fig. 14. Temperature profiles along the DWC.

the external heat requirements and the electricity usage per ton of methanol but still requiring an external heat source (89 kW/ton MeOH) and higher electricity consumption per ton of methanol than in this work (522 vs 472 kWh/ton MeOH accounting only for the hydrogen and recycle compressors).

Wang et al. (2023) recently proposed an alternative that uses a double effect distillation process. Although this is a thermally self-sufficient process that may reduce the power consumption with respect to Kiss et al. (2016) process, it still needs two distillation columns of 40 and 30 trays (compared with one DWC of 29 trays in this work), 21.6 tons of catalyst in the reactor (more than twenty times the amount of catalyst required per kg of MeOH in this work), and the power consumption per ton of methanol is higher than in this work (725 kWh/ton MeOH vs 656 kWh/ton MeOH).

4.4. Economic analysis

After finding an optimized alternative for methanol production by CO_2 hydrogenation, an economic analysis has been performed to analyze whether the production price of methanol by this technology can compete now or in the future with the current selling price of methanol (488 €/ton according to Methanex, 2023).

4.4.1. Capital expenditures (CAPEX)

The calculation of the equipment purchasing cost has been performed using Aspen Capital Cost Estimator V12.0. This proprietary software belongs to AspenTech® and uses a pricing basis that corresponds with the first quarter of 2019. The authors have preferred to use economic data from this year as it belongs to a prepandemic,

Table 6
Comparison of key performance indicators of different methanol production processes by CO_2 hydrogenation.

Parameter	This Work	Kiss et al. (2016)	GhasemiKafrudi et al. (2022)	Meunier et al. (2020)	Pérez-Fortes et al. (2016)	Wang et al. (2023)
MeOH production rate (kton/year)	100	100	100	515	441	100
Purge to feed ratio (mol/mol)	0	0	0	0.005	0	0
Recycle to feed ratio (mol/mol)	4.70	5.47	3.46	n/a	4.69	4.99
H_2:CO_2 ratio (feed/reactor inlet) (mol/mol)	3–3	3–2.84	3–2.11	3–5.3	3–3.8	3/3.92
CO_2 conversion (per pass) (%)	17.40	17.20	21.07	20.10	21.97	22.99
MeOH yield (overall process) (%)	99.99	99.83	99.85	93.40	94.11	99.89
Catalyst load (kg)	865	865	865	156,000	44,500	21,619 [a]
Catalyst load/product MeOH (kgcat/kton/year MeOH)	8.7	8.7	8.7	302.7	101.0	216.2
Power of H_2 feed compressor (kW)	5685	5963	5959	n/a	n/a	6241
Power of CO_2 feed compressor (kW)	2299	–	–	n/a	n/a	n/a
Power of recycle compressor (kW)	212	912	567	n/a	n/a	793
Electricity usage (per ton methanol) (kWh/ton MeOH)	656	550 [c]	522 [c]	331 [b]	305 [b]	725
Electricity usage (per ton methanol) without CO_2 compressor (kWh/ton MeOH)	472	550	522	n/a	n/a	n/a
External heat (kW per ton methanol) (kW/ton MeOH)	0	254	89	0	281	0
Pure CO_2 use (per unit of methanol product) (kg/kg)	1.38	1.38	1.38	1.44	1.46	1.38
Pure H_2 use (per unit of methanol product) (kg/kg)	0.19	0.19	0.19	0.20	0.20	0.19
Column trays	29	4 + 30	4 + 30	30	57	40 + 30

[a] Only void fraction reported (0.5). Mass calculated assuming the same number of tubes and catalyst density as in this work.
[b] Hydrogen feed pressure equal to 30 bar.
[c] CO2 feed pressure equal to 100 bar. No CO2 compressor needed.

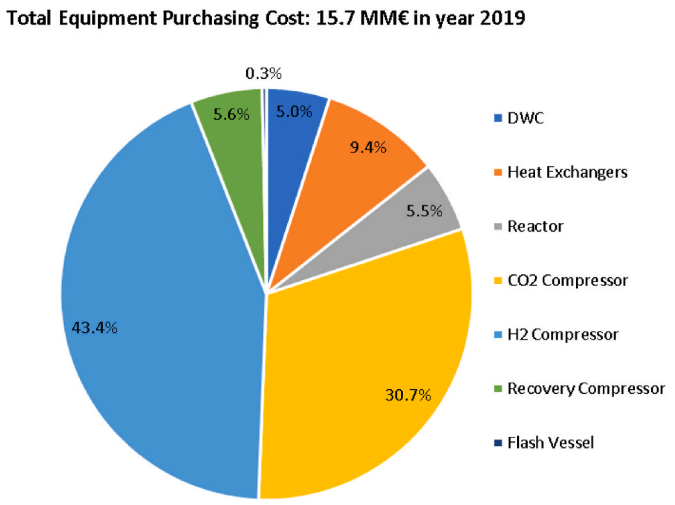

Fig. 15. Equipment purchasing cost for the optimized process.

preinflation context. Thus, no CEPCI cost index correction was applied to update the resulting values. Fig. 15 shows the distribution of the equipment purchasing costs. As can be seen from the figure, the compressors account for almost 80% of the total equipment purchasing costs, the heat exchangers for almost 10%, and the reactor and the DWC for 5% each. The contribution of the rest of the equipment is lower than 0.5%. For a plant of this size, the equipment purchasing cost is equal to 15.8 MM€.

The total investment costs (TIC) are calculated by multiplying the equipment purchasing cost by Lang's factor. A typical Lang's factor of 5 has been selected for this plant, resulting in a TIC of 78.6 MM€.

4.4.2. Operating expenditures (OPEX)

The operating costs of the plant are mainly related to the production of raw materials, the consumption of utilities, the shipping and handling of methanol, the personnel costs, and the general costs. Table 7 shows the OPEX for the optimized process. A current production cost of 1500 €/ton and 85 €/ton for hydrogen and CO_2 respectively and a current electricity price of 0.08 €/kWh have been considered. As can be seen from the table, the total OPEX (58.6 MM€/y) is mainly influenced by the production costs of the raw materials (74% of OPEX).

Table 7
OPEX for the optimized methanol process.

Raw Materials Production Cost		
H_2 Production Cost	1500	€/ton
H_2 Consumption	2650	kg/h
CO_2 Production Cost	85	€/ton
CO_2 Consumption	17,164	kg/h
Total cost of raw materials	43.5	MM€/year
Utilities Cost		
Electricity Price	0.08	€/kWh
Electricity Consumption	9590	kW
Electricity Cost	6.1	MM€/year
Cooling Water Cost	0.3	MM€/year
Utilities Cost	6.5	MM€/year
Shipping and Handling Cost		
Cost per ton of methanol	25	€/ton
Methanol Production	100,000	ton/year
Shipping and Handling Cost	2.5	MM€/year
Variable Costs		
Raw Materials + Utilities + Shipping Cost	52.4	MM€/year
General Costs		
Calculation Factor	10	% Variable Costs
General Costs	5.2	MM€/year
Personnel Cost		
Average Salary + Taxes	60,000	€/year/employee
Number of Employees	15	employees in the unit
Personnel Cost	0.9	MM€/year
Operating Expenditures		
OPEX	58.6	MM€/year

4.4.3. Minimum selling price

The minimum selling price of methanol produced through this process has been obtained by performing a cash flow evaluation based on two typical economic indicators: the net present value (NPV) and the internal rate of return (IRR). The selling price of methanol has been adjusted to obtain a 3% internal rate of return (IRR), which corresponds with a net present value (NPV) of 5 MM€ and a payback time of 8.5 years. All the equations used to calculate the yearly cash flow together with the parameters considered in the evaluation are shown in the *Supplementary Information* file.

The cash flow analysis reveals that the current minimum selling price for methanol produced with this process is equal to 693 €/ton, 42% higher than the current selling price (488 €/ton according to Methanex, 2023).

4.4.4. Sensitivity analysis

Although the minimum selling price of methanol for this process (693 €/ton), cannot compete with the current selling price of methanol (488 €/ton), a sensitivity analysis can reveal how a variation in the main economic drivers of the process affects the NPV. Based on the results obtained in the three previous sections of this work, the sensitivity analysis, shown in Fig. 16, has been done considering as main economic drivers of the process the CAPEX, the hydrogen and CO_2 production cost, and the electricity price. The selling price of methanol has been fixed at the current minimum selling price. As can be seen from Fig. 16, the NPV is mainly influenced by the hydrogen production price, followed by the CO_2 production price, the CAPEX, and the electricity price.

Finally, in a last economic study, it has been quantified how a decrease in the hydrogen and CO_2 production costs and the electricity price affect the minimum selling price of methanol. The minimum selling price is determined under the same basis as in earlier section (selling price adjusted to obtain a 3% IRR). Two new scenarios, named "most probable" and "optimistic" have been considered based on current estimations for future CO_2 and hydrogen production costs (Burdack et al., 2023; Heldebrant et al., 2022). Table 8 shows that for the most probable scenario in the future, the minimum selling price is equal to 587 €/ton, which is 20% higher than the current selling price. If the carbon capture and hydrogen production technologies evolve such that CO_2 can be recovered at a maximum price of 50 €/ton and hydrogen produced by electrolysis at about 1000 €/ton (optimistic scenario), these raw material costs together with cheaper electricity (0.03 €/kWh) and higher fees for CO_2 emissions will mean that the production of e-methanol by CO_2 hydrogenation will compete with the conventional methanol production process by syngas hydrogenation.

4.5. Sustainability metrics

The sustainability of the process was evaluated using several metrics proposed in literature (Sheldon, 2018; Dicks and Hent, 2015): material and energy intensity, E-factor, water consumption, and greenhouse gas (GHG) emissions. These parameters allow a direct comparison with existing processes, with lower values of the indicators representing a better performance of the process.

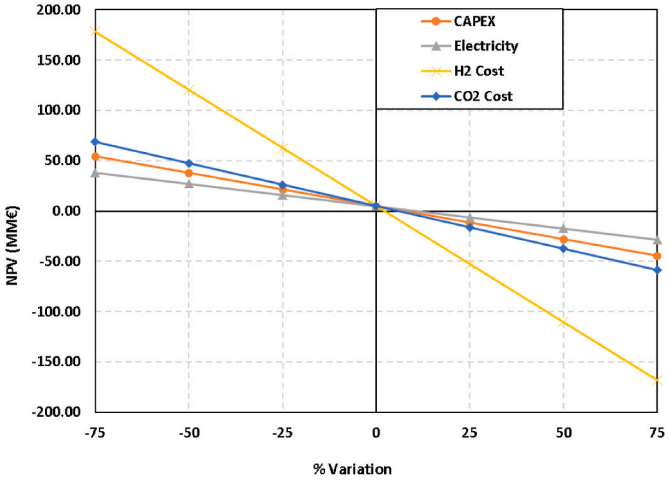

Fig. 16. Economic evaluation: sensitivity analysis.

Table 8
Economic analysis. Methanol minimum selling price.

Scenario	H_2 price (€/ton)	CO_2 price (€/ton)	Electricity Price (€/kWh)	Methanol price (€/ton)
Realistic	1500	85	0.08	693
Most probable	1250	70	0.05	587
Optimistic	1000	50	0.03	481

- *Material intensity*. This parameter is used to measure the total amount of materials required for producing a unit of product. The material intensity of this process is equal to 1.58 kg/kg product, which is derived from the total mass of raw materials (19,813 kg/h) divided by the mass flowrate of methanol produced in the process (12,500 kg/h).
- *E-factor* is used to evaluate the amount of waste produced in the process per kg of products. In the hydrogenation reactor, part of the CO_2 fed to the unit is converted into water (7317 kg/h) instead of being transformed into methanol (12,500 kg/h). Although this water can be reused in the process, for example as cooling water makeup, for E-factor calculation water is considered as a by-product. Thus, the calculated E-factor for this process is equal to 0.58 kg water/kg product.
- *Energy intensity* is a measure of the amount of energy that is consumed per kilogram of products. Since the process is thermally self-sufficient, only the power consumption required in the CO_2, recycling and hydrogen compressors is considered. Since the total power consumption in the compressors of the plant is equal to 8196 kW, the resulting energy intensity is 0.655 $kWh_e/kg_{methanol}$ (2.361 $MJ/kg_{methanol}$). When grey electricity is used instead of green, about 2.5 units of primary energy are required to produce 1 unit of electricity, so the equivalent primary energy requirements are 1.64 $kWh_{th}/kg_{methanol}$.
- *Water consumption.* This metric accounts for the amount of freshwater consumed in the process per kilogram of product. For the calculation of this metric, it is considered that the water streams recovered in the interstage KO drums of the hydrogen compressors and at the bottoms of the distillation column are disposed of instead of being used as e.g. cooling water makeup. Thus, the water consumption in this process is only related to the cooling water consumption in the overhead condenser of the DWC, as the rest of the coolers of the process use air as the cooling agent. Assuming a typical loss of 7% of cooling water in the cooling water tower and a maximum temperature change for cooling water in the cooling water heat exchangers of 10 °C, 73 m^3/h of water are lost in the process. The water consumption in the process is therefore equal to 0.0059 $m^3_{water}/kg_{methanol}$.
- *Greenhouse gas (GHG) emissions.* As the process is thermally self-sufficient and the CO_2, recycling and hydrogen compressors are driven by green electricity, the greenhouse gas (GHG) emissions are limited to those related to the production of electricity and hydrogen, and to the capture of CO_2. When the plant is operated using green electricity and green hydrogen (hydrogen produced by water electrolysis using wind as the power source), the total CO_{2eq} emissions are 0.24 kg_{CO2eq}/kg_{MeOH}. However, if grey electricity (electricity produced from fossil fuels) and grey hydrogen (hydrogen produced by steam reforming of natural gas without carbon capture) are used, the CO_2 emissions increase up to 2.15 kg_{CO2eq}/kg_{MeOH}. Considering that, for a plant of this size, 17,164 kg of CO_2 are consumed every hour, the net CO_{2eq} emissions decrease to −1.13 kg_{CO2eq}/kg_{MeOH} using green hydrogen and electricity and to 0.78 kg_{CO2eq}/kg_{MeOH} using grey hydrogen and electricity. Additional detailed regarding the calculation of the GHG emissions can be found in the *Supplementary Information* file.

The sustainability indicators prove that the process presented here is a clean production route for e-methanol as the CO_2 used is converted at the maximum possible yield to methanol, there is no generation of byproducts and there are no GHG emissions. Compared with previously published works, this process results in a cleaner methanol production route because there is no waste of raw materials (methanol yield is practically 100%), the process is thermally self-sufficient (no

consumption of fuels), and the GHG emissions are limited to those required to produce hydrogen and CO_2 and to those required in the production of green electricity, with the lowest consumption rate per ton of produced methanol (656 kWh/ton_{MEOH}).

5. Conclusions

This work has presented an alternative process for the thermally self-sufficient production of e-methanol by CO_2 hydrogenation with the lowest power requirement per ton of produced methanol of all the works that have been published on this topic. The key findings of this study are presented hereafter.

- The methanol synthesis reaction is best performed in an isothermal reactor operated at 250 °C that provided enough heat to cover all the heat necessities of the process and increased the LMTD of the heat exchangers compared with the operation with an adiabatic reactor. Although it is possible to design a thermally self-sufficient process with an adiabatic reactor, the decrease in the equilibrium yield related to the increase in the outlet temperature must be compensated with an increase in the operating pressure of the reactor. Moreover, lower LMTDs are obtained in the heat exchangers. Operating with an adiabatic reactor with intercooling requires higher investment costs.
- Limiting the pressure decrease in the reaction-separation-recycle loop to the pressure drop of the circuit reduces the overall power consumption to only 656 kWh per ton of methanol (best-in-class) because of the significant reduction of power consumption in the recycle compressor.
- An optimal operating pressure of 65 bar is recommended for the reactor. While operating below this pressure requires larger and more expensive equipment, operating above it increases the equipment thickness and results in more expensive equipment.
- The use of a single-step separation in a DWC allowed for recovering, in a single step, the unreacted CO_2 and obtaining a high purity methanol stream (>99.99% mass). The methanol yield of the process is practically 100%.
- Compared with previously published works, this process consumes less electricity per ton of methanol (656 kWh/ton methanol), is thermally self-sufficient, and obtains high purity methanol (>99.99% wt) at practically 100% yield by only using a single dividing wall column in the separation section.
- From a sustainability perspective, this process does not produce any waste, only water at a production rate of 0.37 $kg_{water}/kg_{products}$, the water consumption is limited to 0.0059 $m^3/kg_{methanol}$, there is no consumption of external fuels, and the GHG emissions are limited to those required for the production of hydrogen, CO_2, and electricity, which is consumed at the lowest rate ever reported (0.655 $kWh_e/kg_{methanol}$). When the plant operates with green hydrogen and electricity, the net CO_2 emissions are negative (−1.13 kg_{CO2}/kg_{MeOH}). If a power backup is needed and the plant operates using grey hydrogen and electricity, the net CO_2 emissions are equal to 0.78 kg_{CO2}/kg_{MeOH}.
- The main two limitations of the process are the fact that an external heat source is needed during the startup of the plant to reach the reaction temperature and that a backup power source is needed if it is not possible to ensure a stable supply of green electricity to the plant.

The combination of methanol isothermal synthesis reactors with the use of a dividing wall column in a heat-integrated process operated at high pressure in the reaction-separation-recycle loop, minimizes the overall production costs of e-methanol by CO_2 hydrogenation. The substitution of the conventional methanol production process by syngas hydrogenation by this cleaner technology will depend mainly on how much the production cost of green hydrogen and the capture cost of CO_2 can be reduced in the future. For example, the current methanol selling price (488€/ton) can be reached with hydrogen production and CO_2 capture costs of 1000€/ton and 50€/ton respectively. However, for the most probable future scenario, the minimum selling price is 587 €/ton, which is ~20% higher than the current selling price.

CRediT authorship contribution statement

Luis Vaquerizo: Conceptualization, Methodology, Formal analysis, Investigation, Visualization, Resources, Writing – original draft, Writing – review & editing. **Anton A. Kiss:** Conceptualization, Methodology, Formal analysis, Investigation, Validation, Visualization, Resources, Supervision, Project administration, Writing – review & editing.

Declaration of competing interest

The authors declare that they have no known competing financial interests or personal relationships that could have appeared to influence the work reported in this paper.

Data availability

Data will be made available on request.

Acknowledgment

Luis Vaquerizo thanks the Spanish Ministery of Universities for the mobility funding (Estancias de Movilidad en el extranjero José Castillejo para jóvenes doctores).

Appendix A. Supplementary data

Supplementary data to this article can be found online at https://doi.org/10.1016/j.jclepro.2023.139845.

References

An, X., Zuo, Y., Zhang, Q., Wang, J., 2009. Methanol synthesis from CO_2 hydrogenation with a Cu/Zn/Al/Zr fibrous catalyst. Chin. J. Chem. Eng. 17, 88–94. https://doi.org/10.1016/S1004-9541(09)60038-0.

Bowker, M., 2019. Methanol synthesis from CO_2 hydrogenation. ChemCatChem 11 (4). https://doi.org/10.1002/cctc.201900401, 238-4,246.

Burdack, A., Duarte-Herrera, L., López-Jiménez, G., Polkas, T.H., Vasco-Echeverri, O., 2023. Techno-economic calculation of green hydrogen production and export from Colombia. Int. J. Hydrogen Energy 48 (1). https://doi.org/10.1016/j.ijhydene.2022.10.064, 685-1,700.

Casale. https://www.casale.ch/technologies/methanol-synthesis-reactor, 2023, 13-June-2023 [WWW Document].

Dang, S., Yang, H., Gao, P., Wang, H., Li, X., Wei, W., Sun, Y., 2019. A review of research progress on heterogeneous catalysts for methanol synthesis from carbon dioxide hydrogenation. Catal. Today 330, 61–75. https://doi.org/10.1016/j.cattod.2018.04.021.

Dicks, A.P., Hent, A., 2015. In: Sharma, S.K. (Ed.), Green Chemistry for Sustainability Green Chemistry Metrics A Guide to Determining and Evaluating Process Greenness, first ed., Springer Briefs in Molecular Science. https://doi.org/10.1007/978-3-319-10500-0

Dieterich, V., Buttler, A., Hanel, A., Spliethoff, H., Fendt, S., 2020. Power-to-liquid via synthesis of methanol, DME or Fischer–Tropsch-fuels: a review. Energy Environ. Sci. 13 (3) https://doi.org/10.1039/d0ee01187h, 207-3,252.

Dimian, A.C., Bildea, C.S., Kiss, A.A., 2014. Integrated Design and Simulation of Chemical Processes, second ed. Elsevier.

Dimian, A.C., Bildea, C.S., Kiss, A.A., 2019. Applications in Design and Simulation of Sustainable Chemical Processes. Elsevier.

Fiedler, E., Grossmann, G., Kersebohm, D., G Weiss, G., Witte, C., 2005. Methanol. In: Ullmann's Encyclopedia of Industrial Chemistry. Wiley-VCH.

GhasemiKafrudi, E., Samiee, L., Mansourpour, Z., Rostami, T., 2022. Optimization of methanol production process from carbon dioxide hydrogenation in order to reduce recycle flow and energy consumption. J. Clean. Prod. 376, 134–184. https://doi.org/10.1016/j.jclepro.2022.134184.

Giampaolo, T., 2010. Compressor Handbook Principles and Practices. The Fairmont Press.

Graaf, G.H., Sijtsema, P.J.J.M., Stamhuist, E.J., Joostes, G.E.H., 1986. Chemical equilibria in methanol synthesis. Chem. Eng. Sci. 41 (2) https://doi.org/10.1016/0009-2509(86)80019-7, 993-2,890.

Heldebrant, D., Kothandaraman, J., MacDowell, N., Brickett, L., 2022. Next steps for solvent-based CO_2 capture; integration of capture, conversion, and mineralisation. Chem. Sci. 13 (6) https://doi.org/10.1039/D2SC00220E, 445-446,456.

Kanuri, S., Roy, S., Chakraborty, C., Datta, S.P., Singh, S.A., Dinda, S., 2022. An insight of CO_2 hydrogenation to methanol synthesis: thermodynamics, catalysts, operating parameters, and reaction mechanism. Int. J. Energy Res. 46 (5), 503–505. https://doi.org/10.1002/er.7562, 522.

Kiss, A. A., Pragt, J. J., van Iersel, M. M., Bargeman, G., de Groot, M. T., Continuous Process for the Preparation of Methanol by Hydrogenation of Carbon Dioxide, Application No. PCT/EP2013/056175, Patent No. WO/2013/144041, EP-2,831,025, Priority date: 28.03.2012.

Kiss, A.A., Process and separation column for separation of methanol, Application No. 12,166,643.2, Patent No. EP-2,660,231, Priority date: 3.05.2012.

Kiss, A.A., Pragt, J.J., Vos, H.J., Bargeman, G., de Groot, M.T., 2016. Novel efficient process for methanol synthesis by CO_2 hydrogenation. Chem. Eng. J. 284, 260–269. https://doi.org/10.1016/j.cej.2015.08.101.

Lee, B., Lee, H., Lim, D., Brigljević, B., Cho, W., Cho, H.S., Kim, C.H., Lim, H., 2020. Renewable methanol synthesis from renewable H2 and captured CO_2: how can power-to-liquid technology be economically feasible? Appl. Energy 279 (115), 827. https://doi.org/10.1016/j.apenergy.2020.115827.

Li, X., Wang, S., Chen, C., 2013. Experimental study of energy requirement of CO_2 desorption from rich solvent. Energy Proc. 37 (1) https://doi.org/10.1016/j.egypro.2013.06.063, 836–1,843.

Lim, H.W., Park, M.J., Kang, S.H., Chae, H.J., Bae, J.W., Jun, K.W., 2009. Modeling of the kinetics for methanol synthesis using Cu/ZnO/Al $_2O_3$/ZrO_2 catalyst: influence of carbon dioxide during hydrogenation. Ind. Eng. Chem. Res. 48 (10) https://doi.org/10.1021/ie901081f, 448–10,455.

Liu, M., Yi, Y., Wang, L., Guo, H., Bogaerts, A., 2019. Hydrogenation of carbon dioxide to value-added chemicals by heterogeneous catalysis and plasma catalysis. Catalyst 9, 275. https://doi.org/10.3390/catal9030275.

Linde, 2023. In: https://www.linde-engineering.com/en/process-plants/hydrogen_and_synthesis_gas_plants/gas_products/methanol/index.html. (Accessed 13 June 2023) (WWW Document).

Lonis, F., Tola, V., Cau, G., 2021. Assessment of integrated energy systems for the production and use of renewable methanol by water electrolysis and CO_2 hydrogenation. Fuel 285 (119), 160. https://doi.org/10.1016/j.fuel.2020.119160.

Matzen, M., Alhajji, M., Demirel, Y., 2015a. Chemical storage of wind energy by renewable methanol production: feasibility analysis using a multi-criteria decision matrix. Energy 93, 343–353. https://doi.org/10.1016/j.energy.2015.09.043.

Matzen, M., Alhajji, M.H., Demirel, Y., 2015b. Technoeconomics and sustainability of renewable methanol and ammonia productions using wind power-based hydrogen. J. Adv. Chem. Eng. 5 (3), 128. https://doi.org/10.4172/2090-4568.1000128.

Matzen, M., Demirel, Y., 2016. Methanol and dimethyl ether from renewable hydrogen and carbon dioxide: alternative fuels production and life-cycle assessment. J. Clean. Prod. 139 (1) https://doi.org/10.1016/j.jclepro.2016.08.163, 068–1,077.

Methanex, 2023. https://www.methanex.com/about-methanol/pricing/, 09-June-2023 [WWW Document].

Meunier, N., Chauvy, R., Mouhoubi, S., Thomas, D., De Weireld, G., 2020. Alternative production of methanol from industrial CO_2. Renew. Energy 146 (1). https://doi.org/10.1016/j.renene.2019.07.010, 192–1,203.

Park, N., Park, M.J., Lee, Y.J., Ha, K.S., Jun, K.W., 2014. Kinetic modeling of methanol synthesis over commercial catalysts based on three-site adsorption. Fuel Process. Technol. 125, 139–147. https://doi.org/10.1016/j.fuproc.2014.03.041.

Pérez-Fortes, M., Schöneberger, J.C., Boulamanti, A., Tzimas, E., 2016. Methanol synthesis using captured CO_2 as raw material: techno-economic and environmental assessment. Appl. Energy 161, 718–732. https://doi.org/10.1016/j.apenergy.2015.07.067.

Porosoff, M.D., Yan, B., Chen, J.G., 2016. Catalytic reduction of CO_2 by H_2 for synthesis of CO, methanol and hydrocarbons: challenges and opportunities. Energy Environ. Sci. 9, 62–73. https://doi.org/10.1039/c5ee02657a.

Ren, M., Zhang, Y., Wang, X., Qiu, H., 2022. Catalytic hydrogenation of CO_2 to methanol: a review. Catalysts 12, 403. https://doi.org/10.3390/catal12040403.

Sheldon, R.A., 2018. Metrics of green chemistry and sustainability: past, present, and future. ACS Sustain. Chem. Eng. 6 (1), 32–48. https://doi.org/10.1021/acssuschemeng.7b03505.

Sollai, S., Porcu, A., Tola, V., Ferrara, F., Pettinau, A., 2023. Renewable methanol production from green hydrogen and captured CO_2: a techno-economic assessment. J. CO2 Util. 68 (102), 345. https://doi.org/10.1016/j.jcou.2022.102345.

Topsoe, 2023. In: https://www.topsoe.com/processes/methanol/synthesis, 13-June-2023 [WWW Document].

Wang, D., Li, J., Meng, W., Liao, Z., Yang, S., Hong, X., Zhou, H., Yang, Y., Li, G., 2023. A near-zero carbon emission methanol production through CO_2 hydrogenation integrated with renewable hydrogen: process analysis, modification and evaluation. J. Clean. Prod. 412 (137), 388. https://doi.org/10.1016/j.jclepro.2023.137388.

Zhong, J., Yang, X., Wu, Z., Liang, B., Huang, Y., Zhang, T., 2020. State of the art and perspectives in heterogeneous catalysis of CO_2 hydrogenation to methanol. Chem. Soc. Rev. 49 (1) https://doi.org/10.1039/c9cs00614a, 385-1,413.